URSI GASS 2021, Rome, Italy, 28 August - 4 September 2021

MUSIC-based Angle-of-Arrival Estimation using Multi-beam Leaky-Wave Antennas

J. Sarrazin
Sorbonne Université, CNRS, Laboratoire de Génie Electrique et Electronique de Paris, 75252, Paris, France
Univ Paris-Saclay, CentralSupelec, CNRS, Laboratoire de Génie Electrique et Electronique de Paris, 91192, Gif-sur-Yvette, France

Abstract

This paper addresses the problem of angle-of-arrival (AoA) estimation with leaky-wave antennas (LWA), specifically, the necessity to operate over large bandwidth to cover a large field of view. By designing the LWA so that multiple space harmonics contribute to the radiation, a multi-beam operation is achieved that allows covering a large angular range using a limited fractional bandwidth. The MUSIC algorithm is then used in order to estimate AoA without ambiguity among the multiple beams. As an example, simulation results show it is possible to estimate AoA over a 180° angular range with a 1.92% bandwidth.

1 Introduction

Angle-of-arrival (AoA) estimation is a key feature in localization systems and channel modeling. Typically, AoA can be estimated using an antenna array and signal processing such as MUSIC algorithm. At the same time, there is a growing interest in the millimeter-wave band for wireless communications. However, at such frequencies, the free space attenuation being severe, an array gain is often required before analog-to-digital conversion, which full-digital array architectures do not benefit from. This can be achieved by sequentially rotating a directional antenna, from which a beamspace MUSIC model can be constructed [1]. The issue with this approach is the scanning duration. Phased arrays offer a much faster electronic beam scanning, at the expense of cost and complexity [2]. An alternative is to use leaky-wave antennas (LWA) that naturally exhibit directional properties while having a main beam that scans the angular space with frequency. This enables having a single-port antenna while benefiting from a large gain, similarly to analog phased arrays except at reduced cost and complexity.

LWAs typically require a large bandwidth to scan a large angular range, i.e., field of view (FoV). Some ways around have been proposed such as using several LWAs [3] [4] or reconfigurable LWA [5], thereby increasing the cost and complexity of the system. This paper proposes to use the radiation of multiple space harmonics in order to scan the FoV with a reduced bandwidth. It is found that MUSIC algorithm can efficiently distinguish sources with different AoA without ambiguity even though the LWA exhibits multiple beams at the same frequency. A system analysis is conducted in order to highlight the benefits of LWA-based AoA estimation and guidelines are given for optimal antenna design. Section 2 discusses the LWA while section 3 introduces the MUSIC system model. Simulation results are shown in section 4 and the conclusion is drawn in section 5.

2 Antenna model

2.1 Background

LWA supports the propagation of a complex guided wave that leaks out of a waveguide into free space. Let us assume a 1D unidirectional periodically modulated LWA leaking through its upper face as depicted in Figure 1. Considering a Floquet mode expansion, the longitudinal wavenumber inside the guiding structure associated with the nth space harmonic is given by:

$$k_z^n = \beta^n - j\alpha \tag{1}$$

where α is the attenuation constant accounting for the leakage as well as the losses and $\beta^n = \beta^0 + 2\pi n/p$ with β^0 the phase constant of the fundamental guided mode and p the spatial period of the modulation. A leaky radiation occurs whenever $-k_0 < \beta^n < k_0$ at a direction given by:

$$\theta_0^n = \sin^{-1}\frac{\beta^n}{k_0} \tag{2}$$

when $\beta \gg \alpha$ and $k_0 = 2\pi f/c$ is the free space wavenumber with c the light velocity. The fact that θ_0^n typically depends on the frequency is used in this paper for AoA estimation. However, to scan the entire FoV $\theta \in [-\pi/2 : \pi/2]$, β^n should span values ranging from $[-k_0 : k_0]$, which typically requires large bandwidth, depending on how fast β^n varies with frequency. Among the fastest scanning LWA to author's bestknowledge, one can cite the work in [6] where a scanning range from $-78°$ to $46.5°$ with a 24% bandwidth (12.25-15.6 GHz) and 30 to 40% total efficiency has been achieved using the $n = -1$ space harmonic radiation. In order to scan the entire FoV with a narrower bandwidth, this paper investigates the use of multiple radiating space harmonics, thereby leading to multi-beam LWA.

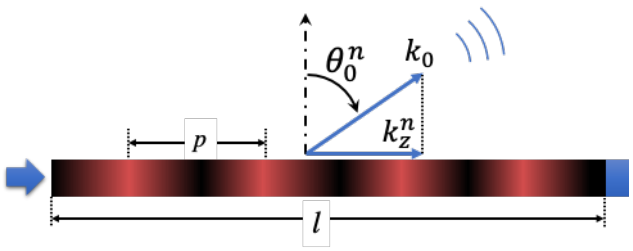

Figure 1. Leaky-wave antenna (input port on the left, matched-load on the right).

2.2 Dispersion analysis and antenna design

Considering a LWA based on a partially open dielectric-filled rectangular waveguide with a periodic modulation small enough not to disturb its operating fundamental mode:

$$\beta^0 = k_0\sqrt{\varepsilon_r}\sqrt{1-(f_c/f)^2} \tag{3}$$

$$f_c = \frac{c}{2a\sqrt{\varepsilon_r}} \tag{4}$$

with ε_r and a the relative permittivity and the width of the waveguide respectively. The waveguide width is chosen such that the minimum operating frequency is $f_{min} = f_c + \delta$, where δ ensures working far enough from the cutoff frequency f_c to avoid severe attenuation in the waveguide. The spatial period p is chosen to ensure angular scanning continuity between the radiation due to each space harmonic:

$$\theta = \sin^{-1}\frac{\beta^n(f_{max})}{k_0(f_{max})} \geq \sin^{-1}\frac{\beta^{n+1}(f_{min})}{k_0(f_{min})} \tag{5}$$

where f_{max} is the maximum operating frequency. To meet the condition in equation 5, the period p should satisfy:

$$p \geq \frac{c\left[1+n_{cont}(1-f_{min}/f_{max})\right]}{f_{min}\sqrt{\varepsilon_r}\left[\sqrt{1-(f_c/f_{max})^2}-\sqrt{1-(f_c/f_{min})^2}\right]} \tag{6}$$

where n_{cont} is the order at which the angular continuity is set between beams due to n and $n+1$ harmonics. Its choice is discussed in section 4. The order of the harmonic radiating at backward end-fire is given by:

$$n_{back} = -\left\lfloor pf_{max}/c\left(1+\sqrt{\varepsilon_r}\sqrt{1+(f_c/f_{max})^2}\right)\right\rfloor \tag{7}$$

where $\lfloor\cdot\rfloor$ is the floor function. The order of the harmonic radiating at forward end-fire is given by:

$$n_{forw} = \left\lfloor pf_{min}/c\left(1-\sqrt{\varepsilon_r}\sqrt{1+(f_c/f_{min})^2}\right)\right\rfloor \tag{8}$$

2.3 Antenna radiation model

In this paper, the radiation of the LWA is approximated with the array factor of a magnetic current line source in free space whose distribution is in the form of a traveling wave [7], here extended to Floquet waves, assuming a periodicity along the line. Assuming all harmonics to be equally excited, an antenna response vector is therefore obtained for the MUSIC system model of the next section as:[1]

$$\mathbf{a}(\theta) = l\sum_{n=n_{back}}^{n_{forw}}\left\{e^{-j(\mathbf{k}_z^n-\mathbf{k}_0\sin\theta)l/2}\mathrm{sinc}\left[(\mathbf{k}_z^n-\mathbf{k}_0\sin\theta)l/2\right]\right\} \tag{9}$$

with l the LWA length, $\mathbf{a}(\theta)$, $\mathbf{k}_z^n$, and $\mathbf{k}_0 \in \mathbb{C}^{M\times 1}$, and M is the number of frequency samples between f_{min} and f_{max}.

3 System Model

The problem considered is the AoA estimation of D received signals that are supposed to be modulated using a multicarrier scheme such as orthogonal frequency-division multiplexing (OFDM). Further assuming that signals on each subcarrier are identical, it is then possible, under narrow-band approximation, to construct a system model similar to spatially-sampled MUSIC to express the received signal due to D plane waves impinging on a LWA in a one-dimensional space as:

$$\begin{bmatrix} x_1[n] \\ \vdots \\ x_M[n] \end{bmatrix} = \begin{bmatrix} a_1(\theta_1) & \dots & a_1(\theta_D) \\ \vdots & \ddots & \vdots \\ a_M(\theta_1) & \dots & a_M(\theta_D) \end{bmatrix} \cdot \begin{bmatrix} s_1[n] \\ \vdots \\ s_D[n] \end{bmatrix} + \begin{bmatrix} z_1[n] \\ \vdots \\ z_M[n] \end{bmatrix} \tag{10}$$

with $\mathbf{x} \in \mathbb{C}^{M\times 1}$, the received data vector, $\mathbf{A} \in \mathbb{C}^{M\times D}$, the LWA response matrix, $\mathbf{s} \in \mathbb{C}^{D\times 1}$, the source vector, $\mathbf{z} \in \mathbb{C}^{M\times 1}$, a complex Additive White Gaussian Noise (AWGN) vector with uncorrelated components, and $n = 1, \dots, N$ is the symbol index (i.e., the nth snapshot among N). Here, equation 10 is a frequency model where M is the number of frequency samples, i.e., number of OFDM subcarriers. Each column of $\mathbf{A}$ represents the LWA response of an incoming plane wave whose AoA is $\theta_{i=1,\dots,D}$ and is given by equation 9.

Assuming $M > D$, N large and always greater than M, and the incoming planes wave not fully correlated, the variance of the i^{th} source AoA estimation can be written as [8]:

$$\mathrm{Var}(\hat{\theta}_i) = \frac{\sigma^2}{2N.h(\theta_i)}\left\{[\mathbf{P}^{-1}]_{ii} + \sigma^2\left[\mathbf{P}^{-1}(\mathbf{A}^*\mathbf{A})^{-1}\mathbf{P}^{-1}\right]_{ii}\right\} \tag{11}$$

where

$$h(\theta_i) = \mathbf{d}^*(\theta_i)\left[I-\mathbf{A}(\mathbf{A}^*\mathbf{A})^{-1}\mathbf{A}^*\right]\mathbf{d}(\theta_i) \tag{12}$$

$$\mathbf{P} = \mathbb{E}\left[\mathbf{x}[n]\mathbf{x}^*[n]\right] \tag{13}$$

and $(\cdot)^*$ denotes the conjugate transpose, $[\cdot]_{ii}$ the ith diagonal element of the related matrix, $\mathbb{E}[\cdot]$ the expectation operator, $\mathbf{d}(\theta_i) = \partial\mathbf{a}(\theta)/\partial\theta|_{\theta_i}$, σ^2 is the average noise power per frequency sample.

[1] the actual LWA pattern depends on the antenna geometry and polarization, and typically exhibits a gain that vanishes towards end-fire.

4 Simulation results

Unless stated otherwise, $\varepsilon_r = 2.9$, $l = 20$ cm, $f_0 = 26$ GHz (central frequency), $\Delta_f = 2$ GHz (bandwidth), $\delta = 0.2$ GHz which sets $a = 3.6$ mm. The attenuation constant is chosen as $\alpha/k_0 = 0.01$.

4.1 Dispersion and radiation pattern of LWA

As a first example, n_{cont} in equation 6 is equal to $n_{forw} - 1$ to satisfy equation 5 for all radiating n. Since n_{forw} in turns depends on p, an iterative approach is conducted to find $n_{forw} = 1$ and $p = 2.62$ cm, which sets $n_{back} = -3$. The obtained dispersion diagram is shown in Figure 2 and the corresponding normalised radiation pattern for a few selected frequencies in Figure 3. In the 25-27 GHz frequency

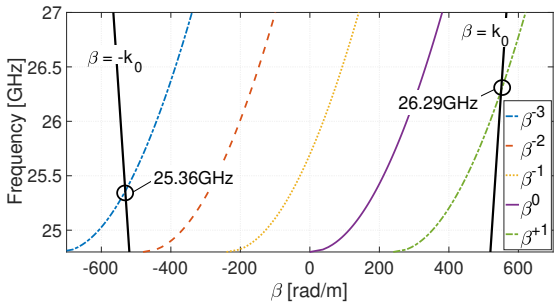

Figure 2. Dispersion diagram.

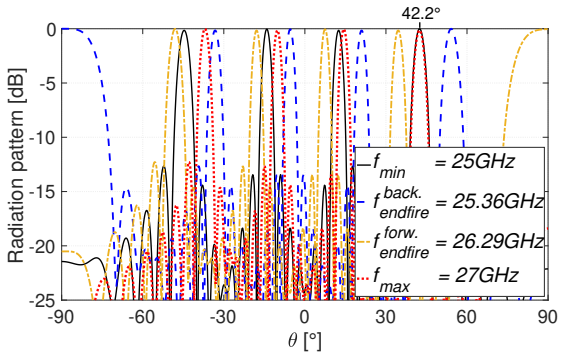

Figure 3. Normalised radiation patterns.

range, it can be observed that a total of $n_{forw} - n_{back} + 1 = 5$ space harmonics (including fundamental mode) lie in the light cone and are therefore responsible for far field radiation. The beam scanning angular continuity can be seen in Figure 3 where the beam due to the fundamental mode ($n = 0$) at 27 GHz is in the same direction ($\theta = 42.2°$) than the beam of the $n = 1$ space harmonic at 25 GHz. Regarding the other beams due to lower-order harmonics, there is an angular overlapping in the scanning: the nth harmonic radiates further (towards positive θ) at 27 GHz than the $n+1$th at 25 GHz. In other words, some directions are covered by more than just one frequency. While this effect is analysed in the next section in terms of AoA estimation, it is also important to note that this has an influence on the antenna design. If n_{cont} in equation 6 is chosen such as $n_{cont} < n_{forw} - 1$, beams due to lower order harmonics will overlap but not those due to higher ones. So on one hand, there might be some angular ranges with less visibility (depending on the beamwidth) but on the other hand, choosing lower value of n in equation 6 decreases the value of the spatial period p, which can ease the practical antenna design. Indeed, having large p value, thereby a fewer number of periods along the antenna length, is not desirable. Radiating a sufficient amount of the traveling wave power will imply a larger modulation index, which in turn typically complicates the impedance matching of the structure. Another solution is to increase the antenna length at the expense of a reduced radiation efficiency due to dielectric and ohmic losses potentially large at millimeter-waves.

To investigate parameters that influence the value of p, Figure 4 shows its variation as a function of fractional bandwidth for two different dielectric constants. Furthermore, the continuity condition in equation 5 is satisfied in one case for all space harmonics by choosing $n_{cont} = n_{forw} - 1$ (like in Figures 2 and 3) and in the other case, for $n_{cont} = n_{back}$. This latter condition means that there is an angular continuity between beams due to n_{back} and $n_{back} + 1$ harmonics but there is no overlapping between beams due to higher ones. It is seen that the larger the bandwidth and/or the greater the permittivity, the smaller the required p value. Furthermore, choosing $n_{cont} = n_{back}$ allows for lower p value, especially when the the permittivity is low. Results in Figure 4 also show that a few-percent fractional bandwidth is sufficient for a multibeam LWA to cover the entire $[-\pi/2 : \pi/2]$ FoV. However, it is to be noted that the LWA should be long enough to allow a modulation over enough spatial periods, which might not be practical for very narrow bandwidth and low permittivity.

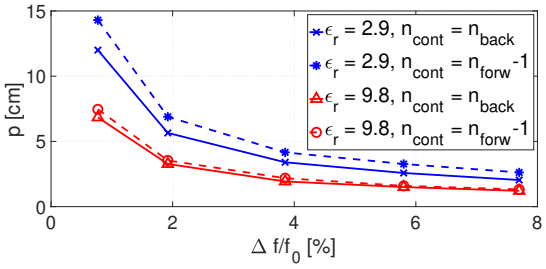

Figure 4. Required spatial period p to cover the $[-\pi/2 : \pi/2]$ FoV as a function of system and antenna parameters.

4.2 MUSIC performance

The MUSIC performance analysis conducted in this section considers $M = 100$, $N = 200$, $\Delta_f = 1$ GHz (3.85%). The signal-to-noise ratio (SNR) is defined as $[\mathbf{P}]_{ii}/\sigma^2 = 0$ dB. The standard deviation obtained with equation 11 is shown in Figure 5 when $D = 1$ (single source). LWA-based results are compared with those obtained from conventional space MUSIC using a $\lambda/2$-spaced-antenna array. It can be observed with the red curves, that a LWA with $\varepsilon_r = 2.9$

and $n_{cont} = n_{forw} - 1$ achieves roughly the same performance than a 26-element array. While $n_{cont} = n_{back}$ may ease the actual design of the LWA (blue curve), it increases the standard deviation, especially where there is no angular continuity. When ε_r gets larger (black curve), the performance gets lower. This is due to the fact that the number of beams to cover the FoV is lower ($n_{forw} - n_{back} + 1 = 7$ when $\varepsilon_r = 2.9$ and $n_{forw} - n_{back} + 1 = 5$ when $\varepsilon_r = 9.8$), each of them scanning more rapidly with the frequency. When M increases to 150 frequency samples (dotted purple curve), the LWA performs like a 30-antenna array (purple curve). It is to be noted that M can be more easily large with LWA (e.g., by decreasing subcarrier spacing in an OFDM scheme) than with conventional array-based MUSIC (i.e., increasing the number of antennas).

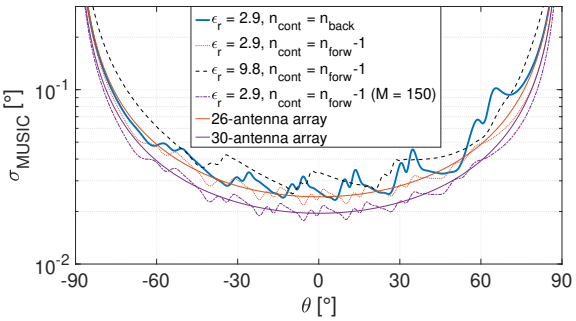

Figure 5. Standard deviation in [°] (SNR = 0 dB, $N = 200$, $f_0 = 26$ GHz, $\Delta_f = 1$ GHz (3.85%).

4.3 MUSIC Pseudo-spectrum

An example of MUSIC pseudo-spectrum is shown in Figure 6 for SNR = 15 dB and $\Delta_f = 0.5$ GHz. $D = 3$ sources are considered at AoA $= [-20°, 24°, 25°]$. It can be observed that the three sources AoA are well estimated and that the system is able to resolve the two close sources at 24° and 25° (the LWA -3-dB-beamwidth is about 3° at these angles). A gap of 10 dB is observed between the spurious peaks and the highest one. It has been empirically observed that this gap level increases with Δ_f. It does also increase with ε_r at the expense of resolvability (larger N values are then necessary to distinguish 24° from 25° AoA).

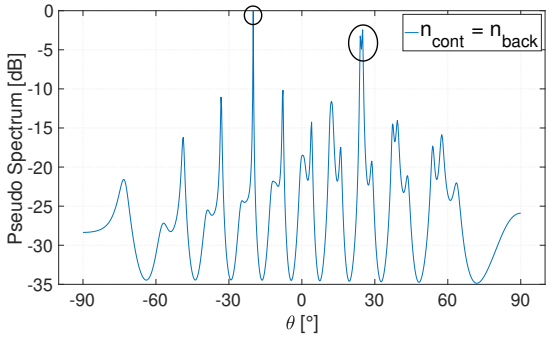

Figure 6. Normalized MUSIC pseudo-spectrum (SNR = 15 dB, $M = 100$, $N = 200$, $\Delta_f = 0.5$ GHz (1.92%).

5 Conclusion

The use of multiple space harmonics in LWA to provide a fast angular scanning is assessed. It is shown that AoA estimation over a large angular range using MUSIC algorithm can be done with a fractional bandwidth as low as a few percents, depending on the antenna technological constraints. This approach reduces system complexity and cost, especially at millimeter-wave, as only one RF chain is required to perform a fast scanning.

6 Acknowledgements

This work was performed within the NOVIS60 project supported by the CEFPRA (Indo-French Center for the Promotion of Advanced Research).

References

[1] C. Ly, H. Dropkin, A. Z. Manitius, "Extension of the MUSIC algorithm to millimeter-wave (MMW) real-beam radar scanning antennas," *Proc. SPIE 4744, Radar Sensor Technology and Data Visualization*, 30, July, 2002, https://doi.org/10.1117/12.488280.

[2] C. U. Bas et al., "Real-Time Millimeter-Wave MIMO Channel Sounder for Dynamic Directional Measurements," *IEEE T-VT*, **68**, 9, Sept. 2019, pp. 8775–8789, doi: 10.1109/TVT.2019.2928341.

[3] M. Poveda-Garcia et Al., "Frequency-Scanned Monopulse Pattern Synthesis Using Leaky-Wave Antennas for Enhanced Power-Based Direction-of-Arrival Estimation," *IEEE T-AP*, **67**, 11, Nov. 2019, pp. 7071–7086, doi: 10.1109/TAP.2019.2925970.

[4] M. K. Emara et Al., "Millimeter-Wave Slot Array Antenna Front-End for Amplitude-Only Direction Finding," *IEEE T-AP*, **68**, 7, July 2020, pp. 5365–5374, doi: 10.1109/TAP.2020.2979284.

[5] H. Paaso, et Al., "DoA estimation through modified unitary MUSIC algorithm for CRLH leaky-wave antennas," *IEEE PIMRC*, London, 2013, pp. 311–315, doi: 10.1109/PIMRC.2013.6666152.

[6] PJ. Liu et Al., "A simple technique for open-stopband suppression in periodic leaky-wave antennas using two nonidentical elements per unit cell," *IEEE T-AP*, **66**, 6, Jun. 2018, pp. 2741–2751, doi: 10.1109/TAP.2018.2819701.

[7] FD. R. Jackson, C. Caloz, and T. Itoh., "Leaky-wave antennas," in *Frontiers in Antennas: Next Generation Design & Engineering*, F. Gross, Ed. New York, NY, USA: McGraw-Hill, 2011, ch. 9, ISBN: 978-0-07-163794-7.

[8] P. Stoica and A. Nehorai, "MUSIC, maximum likelihood, and Cramer-Rao bound," *IEEE T-ASSP*, **37**, 4, May 1989, pp. 720–741, doi: 10.1109/29.17564.